Channel Tracking in Wireless OFDM Systems

Heiko Schmidt, Volker Kühn, and Karl-Dirk Kammeyer
University of Bremen, FB-1,
P.O. Box 33 04 40, D-28334 Bremen, Germany,
e-mail: schmidt@comm.uni-bremen.de
and
Reinhard Rückriem and Stefan Fechtel
Infineon Technologies AG,
P.O. Box 80 09 49, D-81609 Munich, Germany
e-mail: reinhard.rueckriem@infineon.com

Abstract— **In the presented paper, the principle of frequency domain channel estimation for wireless OFDM systems will be shown. A well known noise reduction technique will be adapted to HIPERLAN/2 and IEEE802.11a standards, and its positive effects will be demonstrated by simulation results.**
Channel tracking has not been considered by the WLAN standards named above, although it is well known that time-variant indoor radio channels can change their characteristics within one PHY burst. This paper presents some techniques for decision directed channel tracking, applicable in wireless OFDM systems.

Keywords— **HIPERLAN, IEEE802.11, OFDM, channel estimation, channel tracking, noise reduction**

I. Introduction

The American IEEE802.11a standard and the European equivalent HIPERLAN/2 are two similar concepts for broadband wireless LANs (WLAN) in the 5 GHz band. Both standards are based on the multicarrier modulation technique OFDM (orthogonal frequency division multiplexing) combined with convolutional channel coding. The baseband modulation schemes of both standards are very similar, which simplifies implementation considerably. Challanges and difficulties considered in this paper regard both systems. Except for slight differences in signal mapping, most discrepancies between the standards regard the higher protocol layers.
Section II presents some fundamentals of OFDM and the WLAN standards. Here we focus on the baseband modulation in the PHY layer and explain parts of the PHY burst structure relevant to channel estimation.
Section III describes a frequency domain channel estimator. Assuming channel impulse responses being limited in time, correlations between adjacent subcarriers can reduce the noise influence on the estimated transfer function. Here, a new method for computing the correlations is shown.
In case of time variant channel coefficients, a decision directed channel tracking algorithm for re-estimating the channel coefficients is presented in section IV. The remodulation of the detected data can be done with or without exploiting channel decoding as demonstrated in section IV.

II. Wireless LAN OFDM systems

As mentioned in the introduction, the new WLAN standards HIPERLAN/2 and IEEE802.11a are based on the multi-carrier (MC) technique OFDM [1], [2], [3]. Primarily, OFDM can be described as an analog discrete multitone technique with rectangular (orthogonal) pulse shaping filters for each subcarrier. A guard interval protects the received data against inter-symbol- (ISI) or inter-carrier-interference (ICI). Practically, discrete transmitter and receiver filter banks are used and computed by very efficient FFT algorithms.
Concerning the considered standards, the total OFDM symbol duration is $T = 4$ μs including a $T_g = 0.8$ μs guard interval and the $T_s = 3.2\mu$s core symbol. The $N = 52$ active subcarriers are placed symmetrically (no DC component). With a subcarrier distance of $\Delta f = 1/T_s = 312.5$ kHz the total occupied OFDM bandwidth is about 16.5 MHz. Using an $N_f = 64$ point FFT algorithm (oversampling rate $w = 1.23$), the required time domain sample rate is exactly $f_s = 20$ MHz.

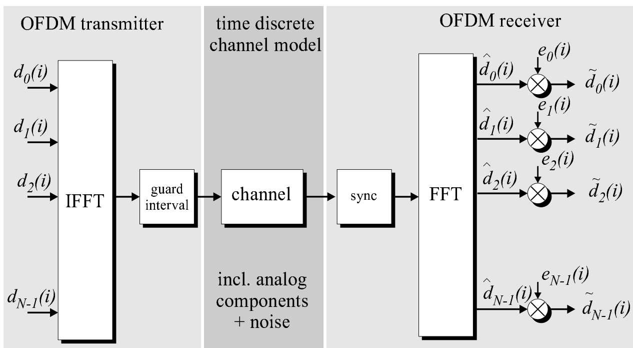

Fig. 1. Time discrete OFDM system

Due to ISI- and ICI-free received symbols, the channel influence can be reduced to one complex Rayleigh fading factor (channel coefficient) on each subcarrier

$$\hat{d}_n(i) = C_n(i) \cdot d_n(i)\,, \tag{1}$$

where $d_n(i)$ denotes the data symbol of the n^{th} subcarrier and the i^{th} OFDM symbol (n: frequency index, i: time index). Assuming a slow fading channel, the transfer function is nearly constant for the duration T of one OFDM symbol. In case of a time invariant channel transfer function,

$C_n = C_n(i)$ describes the belonging coefficients. Since all subcarriers are orthogonal, OFDM needs only one equalizer coefficient for each subcarrier, according to figure 1

$$\tilde{d}_n(i) = e_n(i) \cdot \hat{d}_n(i)\,, \tag{2}$$

normally computed by $e_n(i) = 1/C_n(i)$. This *zero forcing* solution is viable if the channel state information will be considered in the Viterbi channel decoder.
In combination with variable code rates (punctured convolutional codes) and different symbol mapping schemes (BPSK ... 64-QAM), the new WLAN standards provide data rates from 6 up to 54 Mbit/s.
In the PHY layer of HIPERLAN/2 and IEEE802.11a, different burst types with equal training symbols are defined. The preamble contains a synchronisation sequence of 8 μs (except the downlink burst) followed by 2 identical training symbols $d_n^P(i)$ (each 3.2 μs) and protected by one long guard interval. The payload contains user data packets of 432 bit/packet. Figure 2 shows an example PHY burst (27 Mbit/s mode). Each data OFDM symbol consists of 48 data and 4 pilot carriers. The pilot carriers can be used for fine frequency tuning.

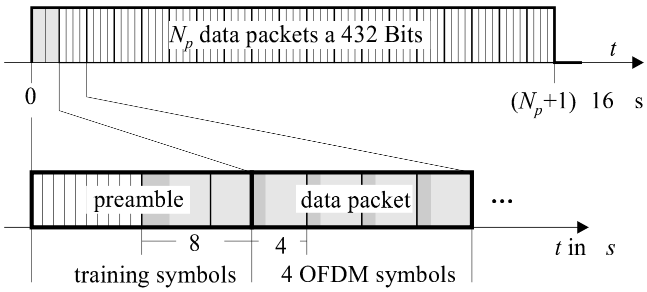

Fig. 2. Time domain burst structure (27 Mbit/s mode)

III. Channel estimation

The presented standards include coherent data demodulation so that the channel has to be estimated. As mentioned in section II, OFDM needs only one coefficient per subcarrier. With the given burst structure, the system permits an estimation using two subcarriers coefficients at the beginning of each burst

$$\hat{C}_n(i) = \frac{\hat{d}_n^P(i)}{d_n^P}\,. \tag{3}$$

With $|d_n^P(i)| = 1$, the division in (3) can be practically replaced by a multiplication with $(d_n^P)^*$. Assuming time invariant channels, the averaged coefficients are

$$\hat{C}_n = \frac{1}{2} \cdot \left(\hat{C}_n(0) + \hat{C}_n(1)\right). \tag{4}$$

Figure 3 shows the block diagram of the channel estimator. In case of AWGN the estimated coefficients are given by the true channel transfer coefficients C_n and additive noise N_n^{ce}

$$\hat{C}_n = C_n + N_n^{ce}\,, \tag{5}$$

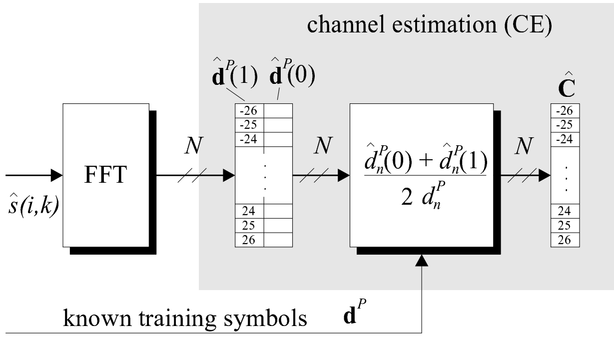

Fig. 3. Initial Channel estimation in frequency domain

where the averaged power of N_n^{ce} is 3 dB below the data symbol distortion (due to averaging over 2 pilot symbols). As simulation results will show, the presented channel estimation method results in an S/N loss of about 2 dB compared to simulations with perfectly known channels.
By exploiting the correlations between adjacent subcarriers coefficients, the estimator noise in (5) can be reduced substantially. The so-called *noise reduction algorithm* (NRA) is placed between IFFT and FFT as shown in figure 4.

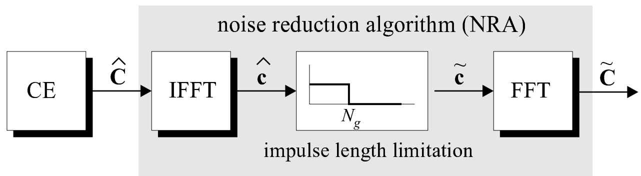

Fig. 4. Noise reduction algorithm (NRA)

In order to fulfill the condition of ISI and ICI free demodulation, the channel impulse response has to match the guard interval. In particular, the maximum channel delay must not exceed the guard time. With the number of guard samples N_g (here: 16), the channel impulse response vector $\mathbf{c}$ of one FFT block with length N_f satisfies

$$c(k) = \begin{cases} \neq 0 & ; \quad 0 \leq k \leq N_g - 1 \\ 0 & ; \quad N_g \leq k \leq N_f - 1 \end{cases}. \tag{6}$$

The estimated channel impulse response $\hat{\mathbf{c}}$ can be computed by an inverse fourier transformation of the estimated channel transfer function vector $\hat{\mathbf{C}}$

$$\hat{\mathbf{c}} = \mathbf{W}_{\mathrm{IDFT}} \cdot \hat{\mathbf{C}}\,, \tag{7}$$

with the IDFT matrix $\mathbf{W}_{\mathrm{IDFT}}$ containing all twiddle factors

$$W_{IDFT}(k,n) = \frac{1}{\sqrt{N_f}} \cdot e^{j2\pi\frac{n \cdot k}{N_f}}\,. \tag{8}$$

The basic idea of noise reduction is the limitation of the impulse response according to

$$\tilde{c}(k) = \begin{cases} \hat{c}(k) & ; \quad 0 \leq k \leq N_g - 1 \\ 0 & ; \quad N_g \leq k \leq N_f - 1 \end{cases}. \tag{9}$$

After re-transformation into frequency domain

$$\tilde{\mathbf{C}} = \mathbf{W}_{\text{IDFT}^{-1}} \cdot \tilde{\mathbf{c}}\,, \tag{10}$$

the averaged noise power in $\tilde{C}_n$ has been reduced by the factor N/N_g. (note: if IDFT and DFT are used for noise reduction, the number of subcarriers N must be equal to the DFT length N_f. Another possibility will be presented in the following text.)

The problem of this well known technique is the computation of the IDFT (7) and the DFT (10) in case of incompletely estimated channel transfer functions. Some of the subcarriers cannot be estimated since they are not used (guard band, DC component) In order to overcome these problems, we can split the vector $\hat{\mathbf{C}}$ into subvector $\hat{\mathbf{C}}_\mathbf{k}$, containing all known or assessable coefficients and subvector $\hat{\mathbf{C}}_\mathbf{u}$ with all unknown channel coefficients. A similar split can also be done in time domain

$$\hat{\mathbf{c}}_\mathbf{1} = [\hat{c}(0), \hat{c}(1), ..., \hat{c}(N_g - 1)]^T\,, \tag{11}$$

$$\hat{\mathbf{c}}_\mathbf{0} = [\hat{c}(N_g), \hat{c}(N_g + 1), ..., \hat{c}(N_f - 1)]^T\,, \tag{12}$$

where $\hat{\mathbf{c}}_\mathbf{1}$ contains the true channel impulse response and $\hat{\mathbf{c}}_\mathbf{0}$ includes zeros (6) or pure noise. The IDFT can be computed by

$$\begin{bmatrix} \hat{\mathbf{c}}_\mathbf{1} \\ \hat{\mathbf{c}}_\mathbf{0} \end{bmatrix} = \begin{bmatrix} \mathbf{W_{11}} & \mathbf{W_{12}} \\ \mathbf{W_{21}} & \mathbf{W_{22}} \end{bmatrix} \cdot \begin{bmatrix} \hat{\mathbf{C}}_\mathbf{k} \\ \hat{\mathbf{C}}_\mathbf{u} \end{bmatrix}, \tag{13}$$

where the IDFT submatrices $\mathbf{W_{11}}$, $\mathbf{W_{12}}$, $\mathbf{W_{21}}$, and $\mathbf{W_{22}}$ include all N_f^2 twiddle factors (8) in a rearranged order. Due to a switched ranking within the frequency domain vector $\hat{\mathbf{C}}$, the rows of $\mathbf{W_k}$ have to be re-organized in the same way. With equation (9), $\hat{\mathbf{c}}_\mathbf{0}$ can be substituted in

$$\hat{\mathbf{c}}_\mathbf{0} = (\mathbf{W_{21}} \cdot \hat{\mathbf{C}}_\mathbf{k} + \mathbf{W_{22}} \cdot \hat{\mathbf{C}}_\mathbf{u})\,, \tag{14}$$

$$\mathbf{W_{22}} \cdot \hat{\mathbf{C}}_\mathbf{u} = -\mathbf{W_{21}} \cdot \hat{\mathbf{C}}_\mathbf{k}\,. \tag{15}$$

With a modified pseudo inverse $\mathbf{W_{22}^+}$

$$\underbrace{(\mathbf{W_{22}^*} \cdot \mathbf{W_{22}} + \gamma^2 \cdot \mathbf{I})^{-1} \cdot \mathbf{W_{22}^*}}_{\mathbf{W_{22}^+}} \cdot \mathbf{W_{22}} = \mathbf{I}\,, \tag{16}$$

the unknown transfer factors can be computed by

$$\hat{\mathbf{C}}_\mathbf{u} = -\mathbf{W_{22}^+} \cdot \mathbf{W_{21}} \cdot \hat{\mathbf{C}}_\mathbf{k}\,, \tag{17}$$

where $\mathbf{I}$ describes the identity matrix. In order to prevent $\mathbf{W_{22}^+}$ from numerical instability, a small factor $0 < \gamma << 1/N_f$ has been introduced. The complete computation of $\hat{\mathbf{c}}_\mathbf{1}$ is

$$\hat{\mathbf{c}}_\mathbf{1} = \left(\mathbf{W_{11}} - \mathbf{W_{12}} \cdot \mathbf{W_{22}^+} \cdot \mathbf{W_{21}}\right) \cdot \hat{\mathbf{C}}_\mathbf{k}\,. \tag{18}$$

Considering (9)

$$\tilde{\mathbf{c}}_\mathbf{1} = \hat{\mathbf{c}}_\mathbf{1}\,, \tag{19}$$

$$\tilde{\mathbf{c}}_\mathbf{0} = \mathbf{0}\,, \tag{20}$$

and with the parts of the resorted DFT matrix

$$\begin{bmatrix} \tilde{\mathbf{C}}_\mathbf{k} \\ \tilde{\mathbf{C}}_\mathbf{u} \end{bmatrix} = \begin{bmatrix} \mathbf{W_{11}^*} & \mathbf{W_{21}^*} \\ \mathbf{W_{12}^*} & \mathbf{W_{22}^*} \end{bmatrix} \cdot \begin{bmatrix} \tilde{\mathbf{c}}_\mathbf{1} \\ \tilde{\mathbf{c}}_\mathbf{0} \end{bmatrix}, \tag{21}$$

with *: transposed conjugate

it is possible to compute the noise reduced subcarrier coefficients

$$\begin{aligned} \tilde{\mathbf{C}}_\mathbf{k} &= \left[\mathbf{W_{11}^*} \cdot \left(\mathbf{W_{11}} - \mathbf{W_{12}} \cdot \mathbf{W_{22}^+} \cdot \mathbf{W_{21}}\right) \cdot \hat{\mathbf{C}}_\mathbf{k}\right] \\ &= \mathbf{W_{kk}} \cdot \hat{\mathbf{C}}_\mathbf{k}\,. \end{aligned} \tag{22}$$

The noise reduction matrix $\mathbf{W_{kk}}$ can be pre-computed offline. Thus, the noise reduction algorithm requires only one run-time matrix multiplication (22). Figure 5 depicts some simulation results of the 27 Mbit/s mode. For Monte-Carlo simulations, a typical Rayleigh fading mobile indoor channel model with a delay spread $\Delta\tau$=100 ns has been chosen. As a reference, the results with perfectly known channel coefficients are given, too.

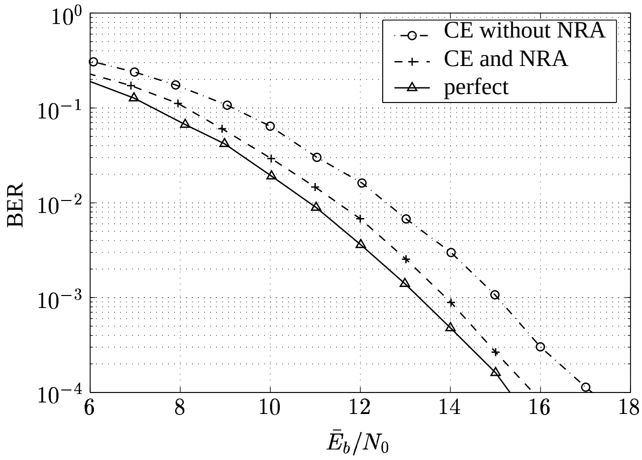

Fig. 5. Simulated bit error rates (BER) with channel estimation (CE) and noise reduction algorithm (NRA)

With raw channel estimation over 2 training symbols (CE without NRA), the E_b/N_0 loss is about 2 dB, compared to perfectly known channels. After re-calculating the subcarrier coefficients by multiplying the noise reduction matrix (22), the E_b/N_0 loss is reduced to 0.7 dB. For other HIPERLAN/2 or IEEE802.11a modes, similar results have been obtained.

IV. Channel tracking

The HIPERLAN/2 and IEEE802.11a standards provide 2 training symbols in front of each data burst and 4 pilot carriers inside each data symbol. In case of time variant channel coefficients, the initial channel estimation suffices only for OFDM symbols near the beginning of the burst. Therefore only 4 pilot carriers are not sufficient to supply channel tracking for a complete subcarrier coefficient set [7].

In order to create additional training symbols, received and decided data can be re-modulated to re-estimate the channel coefficients during data demodulation, as it can be seen in figure 6. The best choice would be decided data feedback from the Viterbi decoder output, because the bit error rate (BER) is much better than at the decoder input. However code termination is only provided at the end of each

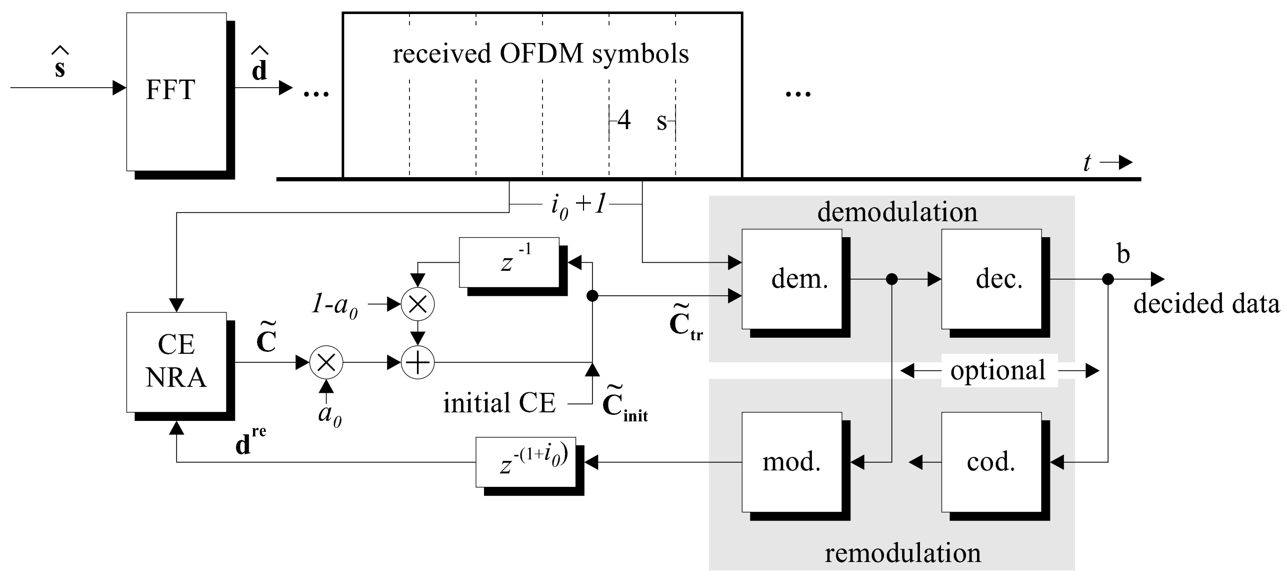

Fig. 6. Block diagram of decision directed channel tracking

data burst. Before code termination has been reached, a sufficiently safe data decision will be at the expense of some Viterbi decision delay. Figure 7 shows the simulated bit error rates subjected to the decoding delay $k_{\mathbf{max}}$ with different coding rates R_p.

The results of figure 7 are summarized in table I for all HIPERLAN/2 modes. In a worst case scenario with $R_p = 3/4$, the Viterbi decoder needs a delay of 100 decoded bits. With 1 OFDM symbol containing 36 data bits (9 Mbit/s mode), a maximum decoding delay of $i_0 = 3$ complete OFDM symbols is required. In order to obtain comparable results, this delay has been used for all modes.

The other feedback possibility is to use the non decoded symbols at the symbol decoder output for re-modulation ($i_0 = 0$). Figure 6 demonstrates both options.

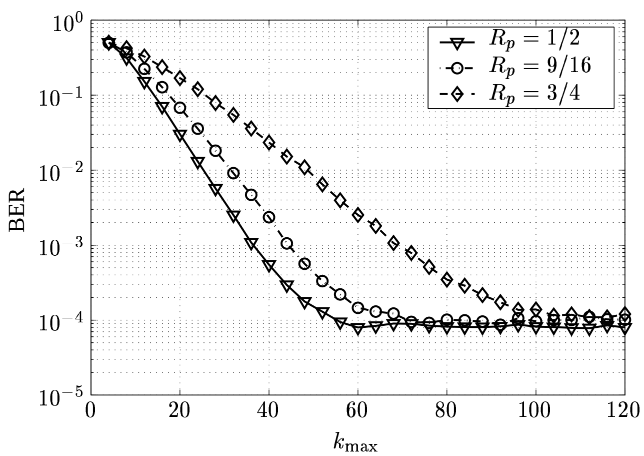

Fig. 7. simulated bit error rates (BER) of 27 Mbit/s mode versus decoding delay $k_{\mathbf{max}}$ (only AWGN)

Mode	R_b	N_{bps}	$k_{\max}$	$\min(i_0)$	Δt_{dec}
6	1/2	24	> 60	3	12 μs
9	3/4	36	> 110	3	12 μs
12	1/2	48	> 60	2	8 μs
18	3/4	72	> 110	2	8 μs
27	9/16	108	> 70	2	8 μs
36	3/4	144	> 110	1	4 μs
54	3/4	216	> 120	1	4 μs

TABLE I
Estimated decoding delay

The first $i_0 + 1$ OFDM symbols are demodulated by using the initial channel estimation. The decided data (before or after decoding) must be re-modulated. The decision delay is modulated by $z^{-(1+i_0)}$. Dividing $\hat{\mathbf{d}}(i)$ by $\mathbf{d^{re}}(i)$ and applying the noise reduction algorithm will produce a new channel estimation $\tilde{\mathbf{C}}(\mathbf{i})$ for the i^{th} OFDM symbol. In order to reduce noise influence, a first order loop filter with parameter $a_0 < 1$ has been introduced, as shown in figure 6.

Finding an optimal loop parameter a_0 is a compromise between noise sensitiveness and tracking power. In order to simulate the noise influence, a time-invariant Rayleigh-fading indoor channel model ($\Delta\tau = 100$ns) has been used. Figure 8 shows the simulated BER versus a_0 for both cases: decided data feedback before (uncoded) and after Viterbi decoding (coded). The averaged noise power is $\bar{E}_b/N_0 = 15$ dB.

In case of $a_0 = 0$, no tracking will be done and the BER must be identical to that in figure 5 with NRA. Of course, with an increased a_0, the noise influence on tracking based on non-decoded reference symbols rises more than for decoded symbols. With $a_0 < 0.2$ (uncoded) and $a_0 < 0.5$ (coded) a negligible BER loss can be obtained.

For tracking power simulations, a time variant channel model has been used, considering Jakes-distributed Doppler-

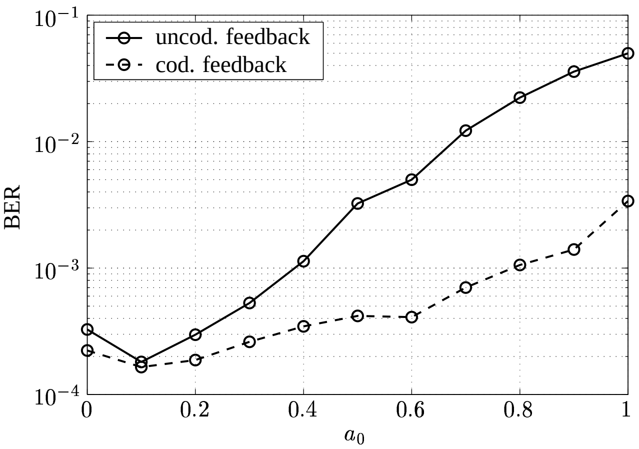

Fig. 8. Simulated bit error rates (BER) of 27 Mbit/s mode versus loop parameter a_0 with $\bar{E}_b/N_0 = 15\text{dB}\}$

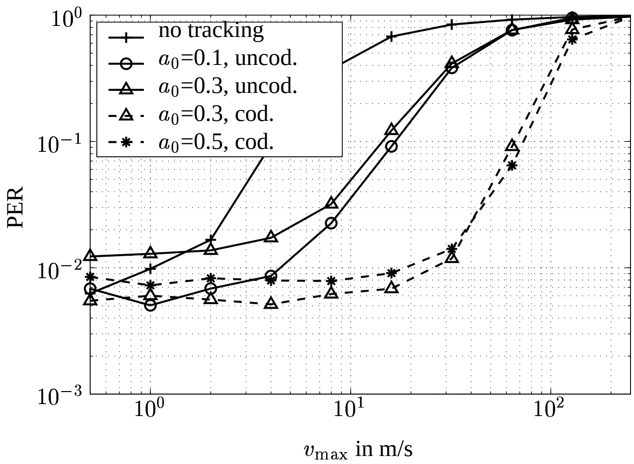

Fig. 9. Simulated packet error rates (PER) of 27 Mbit/s mode versus object speed $v_{\mathbf{max}}$ with $\bar{E}_b/N_0 = 15$

spreading derived from mobile speed $v_{\mathbf{max}}$

$$f_{D,\mathbf{max}} \approx \frac{1}{\lambda} \cdot v_{\mathbf{max}} \tag{23}$$

with wave length $\lambda = \frac{c_0}{f_0}$ (here $\lambda = 5.77 \cdot 10^{-2}$m).
In figure 9 the simulated packet error rates (PER) of a HIPERLAN/2 system (27 Mbit/s) in case of high mobility is depicted. The simulated PHY burst length is about 800 μs. Without tracking, the PER becomes very high for more than 3 m/s. Applying channel tracking after exploiting Viterbi decoding, the system functionality can be guaranteed up to $v_{\mathbf{max}} = 30$ m/s.

V. Conclusions

In section II, the PHY layer of modern wireless LAN standards in 5 GHz band has been presented. Here we focused on OFDM fundamentals and the PHY burst structure. The training symbol constellations of HIPERLAN/2 and IEEE802.11a are equal.
Section III shows a frequency domain based channel estimation. The influence of noise can be reduced by applying the noise reduction algorithm (NRA). It is based on a time limited channel impulse response. By permutating the IDFT matrix, the run-time costs of the NRA can be reduced to one matrix multiplication. The gain of about 1.3 dB has been verified by simulation results.
In case of time variant channel coefficients, channel tracking is necessary. Thus, a channel tracking scheme, applicable to HIPERLAN/2 and IEEE802.11a, has been presented in section IV. With Viterbi decoding placed inside the feedback loop, the channel estimation based on re-coded and re-modulated symbols yields better results. Although the Viterbi decoder needs a decoding delay, channel tracking with exploitation of channel decoding permits higher Doppler frequencies and thus higher mobile speeds.
This paper has shown an efficient method to estimate the subcarrier coefficients. Furthermore, the necessity of channel tracking has been demonstrated and a practical solution has been presented.

References

[1] ETSI. HIPERLAN Type 2 Functional Specification Part 1 – Physical PHY Layer. Technical Report DTS/BRAN030003-1, ETSI EP BRAN, April, 2000.
[2] IEEE. Draft Supplement to STANDARD for Information Technology-Telecommunications and information exchange between systems – Local and metropolitan area networks – Specific Requirements – Part 11: Wireless LAN Medium Access Control MAC and Physical Layer PHY specifications: High Speed Physical Layer in 5 GHz Band. Technical Report IEEE P802.11a/D7.0, IEEE, 1999.
[3] M. Johnsson. HiperLAN/2 - The Broadband Radio Transmission Technology Operating in the 5 GHz Band. *HiperLAN/2 Global Forum (www.hiperlan2.com)*, 1999. Version 1.0.
[4] J. G. Proakis. *Digital Communications*. McGraw-Hill, 3. edition, 1995.
[5] K. D. Kammeyer. *Nachrichtenübertragung*. B.G.Teubner, Stuttgart, 2. edition, 1996.
[6] H. Meyr, M. Moeneclaey, and S. A. Fechtel. *Digital Ccommunication Receivers*. John Wiley, 1. edition, 1998.
[7] M. Feuersänger, H. Schmidt, and K.D. Kammeyer. An Iterative Channel Estimation for a Hiperlan/2 OFDM System. In *Proc. of 5. international OFDM Workshop*, Hamburg-Harburg, Germany, September 2000.
[8] H. Schmidt. *OFDM für die drahtlose Datenübertragung innerhalb von Gebäuden*. PhD thesis, University of Bremen, Germany, Arbeitsbereich Nachrichtentechnik, Shaker Verlag, April 2001.
[9] R. van Nee und R. Prasad. *OFDM for Wireless Multimedia Communications*. Artech House Publishers, Boston, London, 2000.